ACS APPLIED MATERIALS & INTERFACES

Research Article

www.acsami.org

# Hierarchically Self-Organized Monolithic Nanoporous Membrane for Excellent Virus Enrichment

Gumhye Jeon,[‡,†] Minhyeok Jee,[§,†] Seung Yun Yang,[⊥] Bom-yi Lee,[‡] Sung Key Jang,*[,§] and Jin Kon Kim*[,‡]

[‡]National Creative Research Center for Smart Block Copolymers, Department of Chemical Engineering, [§]Molecular Virology Laboratory, POSTECH Biotech Center, Department of Life Science, Pohang University of Science and Technology, Pohang, Kyungbuk 790-784, Republic of Korea

[⊥]Department of Biomaterials Science, Pusan National University, Miryang, Gyeongnam 627-706, Republic of Korea

Supporting Information

**ABSTRACT:** Enrichment of viruses is essential for making high dose viral stocks for vaccines and virus-related research. Since the widely used ultracentrifugation for concentrating viral stock requires ultra-high speed rotation, it easily destroys the activity of some viruses, for instance, hepatitis c virus (HCV), which has a fragile structure and low virus titer. We introduce a novel method to concentrate HCV virus in stock by using a hierarchically self-organized monolithic nanoporous membrane made by stepwise anodization. The pores at the top part of the membrane have very regular sizes that are suitable for the perfect filtration of the virus particles in the stock. On the other hand, the remaining part has large pores that maintain high flux and mechanical strength of the membrane under the high pressure (up to 10 bar). The enrichment efficiency of HCV in crude stocks by using the membrane became over 91%, which is four times higher than that (~22%) obtained by conventionally used centrifugation. A very high efficiency results from the perfect filtration and no damage to the virion particles during the enrichment process, whereas significant damage to the HCV occurs during centrifugation. The hierarchically self-organized monolithic nanoporous membrane could be effectively employed for concentrating various fragile viruses in stocks, for instance, rabies virus and human immunodeficiency virus in addition to HCV virus.

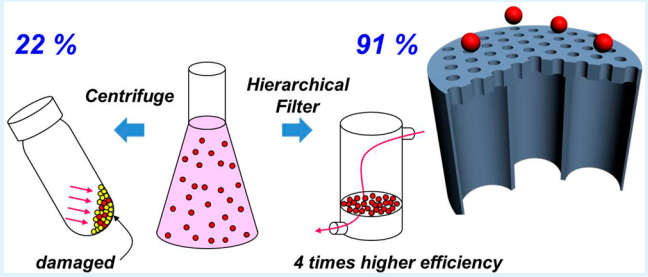


**KEYWORDS:** *nanoporous membrane, hierarchical structure, monolithic structure, virus enrichment, hepatitis C virus*

## INTRODUCTION

Viruses such as human immunodeficiency virus (HIV), severe acute respiratory syndrome (SARS) coronavirus, and avian influenza virus (type H5N1) are the major pathogens that cause the serious diseases of acquired immune deficiency syndrome (AIDS), SARS, and acute respiratory distress syndrome (ARDS). To develop therapeutic agents or vaccines against these viruses, virus cultivation should be a prerequisite. However, viral yields (or titers) generated from *in vitro* cultivation vary greatly depending on the viruses. For picornaviruses, such as poliovirus, the plaque forming unit (pfu) could reach ~$10^{11}$ pfu/mL.[1] On the other hand, poorly growing viruses, for instance, hepatitis c virus (HCV), often yield less than $10^2$ focus-forming units (FFU)/mL.[2]

For a virus with lower titers, its enrichment in stocks is required for basic research and vaccine developments. For instance, high titer virus is needed for the investigation of the virus proliferation cycle. Inoculation of virion particles of more than 5 multiplicity of infection (5 MOI) per cell is needed to make simultaneous infection of cells more than 99%.[3] Moreover, highly concentrated virus stocks are recommended for storage and delivery of vaccines to patients, which are required to be cold or frozen.

Virion particles have often been enriched (or concentrated) by filtration through an ultrafine filter (Amicon Ultra: Millipore) or by ultracentrifugation of viral stocks.[3] However, a significant loss of virions by leakage through the membrane and the deterioration of virus infectivity through virus damage during ultracentrifugation prevent the effective enrichment of virus stocks. Therefore, it is of the utmost importance to develop a facile and effective method (or system) to concentrate virus stocks without loss and damage of the virus.

In this study, we chose HCV as a model virus for virus enrichment, since its viral titer is very low and it is labile in culture media.[4] HCV causes various liver diseases such as hepatitis, liver cirrhosis, and hepatocellular carcinoma.[5] The understanding of the HCV life cycle and pathogenesis has been hampered by the lack of finding a satisfactory culture system.[6] Although the HCV cell culture system has been developed recently, the *in vitro* cultivation system produces low-titer infectious virions.[7] Therefore, HCV in stocks should be enriched for the development of drugs and vaccines against *infectious* HCV. Enrichment of HCV in stocks has often been

Received: November 5, 2013
Accepted: December 19, 2013
Published: December 19, 2013





dx.doi.org/10.1021/am4049404 | ACS Appl. Mater. Interfaces 2014, 6, 1200−1206

achieved by precipitation of virion particles in a cell culture medium through centrifugation at an ultra-high speed (for instance, 36 400 rpm),[8,9] but the efficiency of HCV enrichment is quite low.

We hypothesize that a low efficiency arises mainly from a loss or damage of HCV virions during ultra-high speed centrifugation. Once a filtration process via nanoporous membranes is employed, the damage to the virus is effectively prevented and the efficiency would be increased. For this purpose, various nanoporous membranes can be used, for instance, track-etched polycarbonate (PC) membranes, commercially available anodic aluminum oxide (AAO) membranes, and block copolymer membranes.[10−24]

Although track-etched PC membranes have high selectivity due to uniform pore size, they show very low flux due to low pore density and long separation layer.[13] Commercially available AAO membranes give high flux, but they show low selectivity due to nonuniform pore size. To design nanoporous membranes for excellent virus enrichment in stocks, the pore size should be uniform and smaller than the diameter of virion particles. They should also exhibit high flux, excellent selectivity, sterilizability, and long-term filtration stability. To achieve these requirements, inorganic membranes with superior mechanical and thermal stabilities than polymer-based membranes are required. Also, the monolithic nanoporous structure shows excellent mechanical stability. The top layer in the membrane should have uniform pore size for perfect filtration of viruses in stocks, and the channel length should be short to provide high flux. The remaining layer should have larger pore sizes and long enough channel length to provide excellent mechanical strength without sacrificing high flux.

Yamaguchi et al. prepared a hierarchically nanoporous structure by adding mesoporous silica into an AAO membrane.[14,15] Though this membrane had a hierarchical nanoporous structure, the filtration layer was too thick (5−20 $\mu$m). Previously, we prepared a nanoporous composite membrane with a diameter of ∼15 nm and uniform pore size based on block copolymer self-assembly, followed by placing it on a commercially available microfiltration membrane.[16−19] This membrane showed high flux and excellent selectivity for the filtration of human rhinovirus.[16] However, this composite membrane could not be used for effective enrichment of virion particles due to poor mechanical strength under the high pressure and many fabrication steps including floating of the film. Besides, nanoporous membranes with monolithic structure are more suitable than a composite membrane for better mechanical stability of the membrane.

Some research groups fabricated membranes with hierarchical nanoporous structures based on phase inversion of a block copolymer in a nonsolvent.[20−24] However, the membranes occasionally contained large sized pores and thus could not be used for enrichment of virion particles. The biggest problem is that the polymeric nanoporous membranes do not show sterilizability, which is an essential step in enrichment of the viruses in stock, because the concentrated virus stock should not contain any microorganisms such as bacteria and viruses. However, polymeric nanoporous membranes are not stable under the high temperature and pressure needed for sterilization.

Here, we fabricate a hierarchically self-organized monolithic nanoporous membrane by sequential anodization of aluminum. It has ideal structure for filtering and concentrating some viruses, because of high flux, excellent selectivity, long-term stability, and sterilizability. While both a commercial AAO membrane (e.g., Anodisc) and the membrane employed in this study show hierarchically structured nanopores, the former has a broad pore size distribution in the skin layer. On the other hand, the latter shows very uniform pores in the skin layer. This is because two different but constant applied potentials during anodization were used to fabricate small and uniform pores on preexisting large pores. With this membrane, HCV virions in stocks are effectively concentrated without a loss of virus infectivity. On the other hand, when the most frequently used method, filtration with an ultrafiltration membrane (Amicon Ultra: Millipore) followed by ultracentrifugation, is employed for the concentration of HCV viruses in stock, the efficiency of concentrating HCV virus is very low (∼22%) due to loss of viruses and significant damage in virus infectivity.

## EXPERIMENTAL SECTION

**Preparation of the Hierarchically Self-Organized Monolithic Nanoporous Membranes.** A hierarchically self-organized monolithic nanoporous membrane was fabricated by stepwise anodization. An aluminum sheet (99.999%, 1 mm thickness) was electropolished in the mixture of perchloric acid and ethanol (1:4 v/v) at 7 °C and 20 V. Anodization was carried out for 16 h in 0.1 M phosphoric acid aqueous solution under an applied potential of 195 V. At the end of the first anodization, pore widening was carried out for 4 h at 30 °C in 0.1 M phosphoric acid. Then, the voltage was dropped to 30 V to prepare smaller pores.[25−29] After a further widening process for 5 h, anodizing at 30 V was conducted in oxalic acid (0.3 M) at 10 °C for various times. Aluminum was removed using $CuCl_2$ aqueous solution. The fabricated aluminum oxide layer was protected by poly(vinyl chloride) film during the chemical etching. Then, the aluminum oxide barrier layer was opened with inductively coupled plasma etching with $BCl_3$ gas for 110−130 s at a flow of 75 sccm, a pressure of 5.0 mTorr, a bias power of 200 W, and a source power of 300 W. Morphology of the nanoporous membrane was investigated by field emission scanning electron microscopy (FESEM, Hitachi S-4800) that operated at 3 keV.

**Cell Culture and Enrichment of HCV in Stock.** The human hepatoma cell line Huh 7.5.1 cells were cultured in Dulbecco's modified Eagle's medium (DMEM; Invitrogen) supplemented with 10% fetal bovine serum (FBS; HyClone), penicillin, and streptomycin.[30] *Infectious* HCV was produced by the electroporation of Huh 7.5.1 cells with *in vitro*-transcribed HCV RNA. After three days, cultured media were harvested at every 12 h.

The culture media (5 mL) of each HCV infected cell in 100 mm plates was collected and filtered by 0.2 $\mu$m syringe filter to remove any cell debris. The volume of media (100 mL) was reduced about one quarter with an ultrafiltration membrane (Amicon Ultra 100K) under centrifugation at a low rotating speed (3300 rpm). Then, the centrifuged media (27 mL) was loaded onto a 20% sucrose cushion in an ultracentrifuge tube. The HCV particles were enriched by centrifugation at 36 400 rpm for 4 h at 4 °C in a Beckman SW45Ti rotor. The pellet was washed by phosphate buffered saline (PBS) and resuspended in 1.0 mL of DMEM. The filtering process for the enrichment was performed by using the hierarchically self-organized monolithic nanoporous membrane (area of 2 $cm^2$) with a skin layer with a thickness of 100 nm at 4 °C and $\Delta P$ = 3 bar under a dark environment, and 100 mL of original HCV virus supernatant was enriched to 1 mL.

**Flux Measurement.** Water flux was measured at various pressures ($\Delta P$) from 1 to 4 bars at room temperature by using an amicon stirred cell. The area of the hierarchically self-organized monolithic nanoporous membrane was 2 $cm^2$. Pressure was applied by nitrogen gas controlled with a regulator and barometer. The amount of the ejected water was automatically weighed every 5 s. A homemade flux cell with stainless steel was used for water flux at high pressure (say 10 bar).

**Determination of HCV Titer (ICC).** For fluorescence microscopic analysis, Huh 7.5.1 cells on gelatin coated 25 mm glass were fixed in

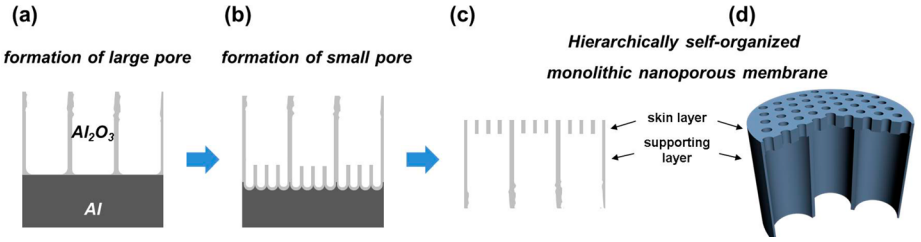


**Figure 1.** Schematic for the fabrication of a hierarchically self-organized monolithic nanoporous membrane. (a) Large pores are fabricated and used as a supporting layer. (b) The skin layer with small and regular pores is sequentially prepared on preexisting large pores. (c) The hierarchically structured nanoporous membrane is obtained after removal of the barrier layer. (d) Stereoscopic view of hierarchically self-organized monolithic nanoporous membrane.

4% paraformaldehyde for 10 min and then permeabilized by 0.01% Triton X-100 in PBS for 2 min. HCV infected hepatocytes were analyzed using an HCV core antibody. Each glass was incubated with a blocking solution (1% bovine serum albumin (BSA) in PBS) at room temperature for 30 min, followed by an additional incubation with monoclonal antibody against core (1:400 dilution; Fisher Scientific). After washing three times with PBS, specific binding was detected with Alexa 488-labeled anti-mouse IgGs (Molecular Probes; 1:200 dilution). The foci of HCV positive cells were counted using a fluorescence microscope and software.

**Quantification of HCV RNA.** Total RNAs were extracted using Trizol-LS solution according to the manufacturer's instruction. Complementary DNAs to the HCV were synthesized using Takara Reverse transcriptase according to the manufacturer's protocol.[31] Quantification of viral RNA was done by a Biorad IQ5 multicolor real-time PCR detection system by using two-step RT-PCR and SYBR Green detection. RNA copy number was calculated by using cycle threshold values.

## RESULTS AND DISCUSSION

**Performance of Membrane.** A hierarchically self-organized monolithic nanoporous membrane was prepared by continuous stepwise anodization of aluminum, as shown in Figure 1. First, large pores used as a supporting layer of the membrane were fabricated on an aluminum sheet by anodization at a high potential (Figure 1a).[32−36] Since the pore size was ∼450 nm, it was much larger than the diameter of HCV virus. Thus, to perfectly filter HCV viruses, smaller pores than the diameter of HCV virus (∼50 nm) have to be prepared. These smaller pores are fabricated by applying a low voltage of 30 V on the preformed larger pores (Figure 1b). The thickness of the skin layer with smaller pores is easily controlled by varying the anodizing time. After removing the aluminum substrate by chemical wet-etching with copper chloride, the barrier layer touching the aluminum substrate was removed by dry-etching to avoid unwanted pore widening of the skin layer. The skin (or top) layer of the membrane was used for the filtration of the viruses in stocks. Thus, a hierarchically self-organized monolithic nanoporous membrane has smaller pores in the top layer and larger pores in the remaining membrane (Figure 1c,d).

Figure 2 gives SEM images of the hierarchically self-organized monolithic nanoporous membranes after various anodization times of the second anodization step. The pore size and thickness of the supporting layer are fixed as 450 nm and 70 $\mu$m, respectively. While the pore size of the skin layer was the same (23 ± 2 nm), the thickness of the skin layer decreased from 500 to 100 nm with decreasing anodization time from 18 to 4 min. The hierarchically self-organized monolithic nanoporous membrane has higher pore density and more regular pore size compared with commercially available membranes, for

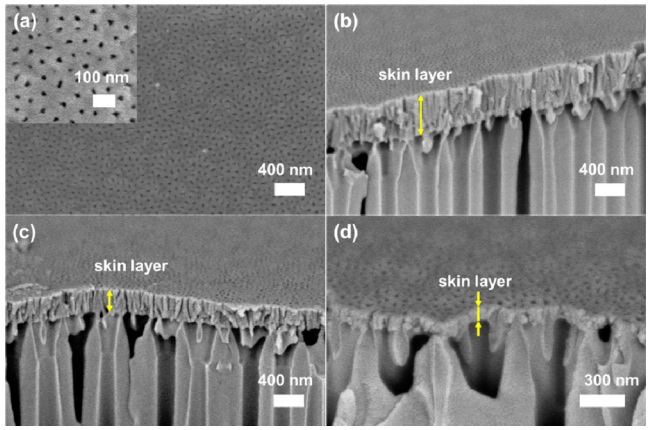


**Figure 2.** (a) Top and (b−d) cross-sectional SEM images of the hierarchically self-organized monolithic nanoporous membranes prepared by different anodization times (min) of the second anodization step: (b) 18; (c) 9; (d) 4.

instance, AAO membrane and track-etched PC membrane (see Figure S1 in the Supporting Information). Because the diameter of an HCV virus particle is ∼50 nm, HCV would be completely filtered by the hierarchically self-organized monolithic nanoporous membrane.

Figure 3 gives plots of flux ($J$) versus applied pressure ($\Delta P$) for the hierarchically self-organized monolithic nanoporous membranes having various thicknesses of the skin layer. The flux data for a commercially available PC membrane was added for the reference. Here, the thickness of the skin layer ($h_{skin}$) was changed, while the pore size in the skin layer was kept the same. Also, the pore size and thickness of the supporting layer ($h_{support}$) were fixed. The flux of a nanoporous membrane with $h_{skin}$ of 250 nm was 1200 $Lm^{-2}h^{-1}$ at $\Delta P$ = 3 bar, which is 12 times higher than that (100 $Lm^{-2}h^{-1}$) of the commercial track-etched PC membrane.

To investigate the mechanical stability of the membrane under high pressure (e.g., 10 bar), we performed a water flux experiment by increasing pressure up to 11 bar. For this purpose, we fabricated a homemade stainless steel membrane housing. As shown in the inset of Figure S2a, Supporting Information, the flux of deionized water increased linearly with $\Delta P$. This indicates that the hierarchically nanoporous structure of the membrane is well maintained even at $\Delta P \sim 11$ bar. To provide a direct evidence of mechanical stability of the nanoporous membrane after a flux experiment at higher $\Delta P$, we observed, via SEM, the membrane surface after the flux experiment. We do not find any crack on the surface of membrane, as shown in Figure S2b, Supporting Information.

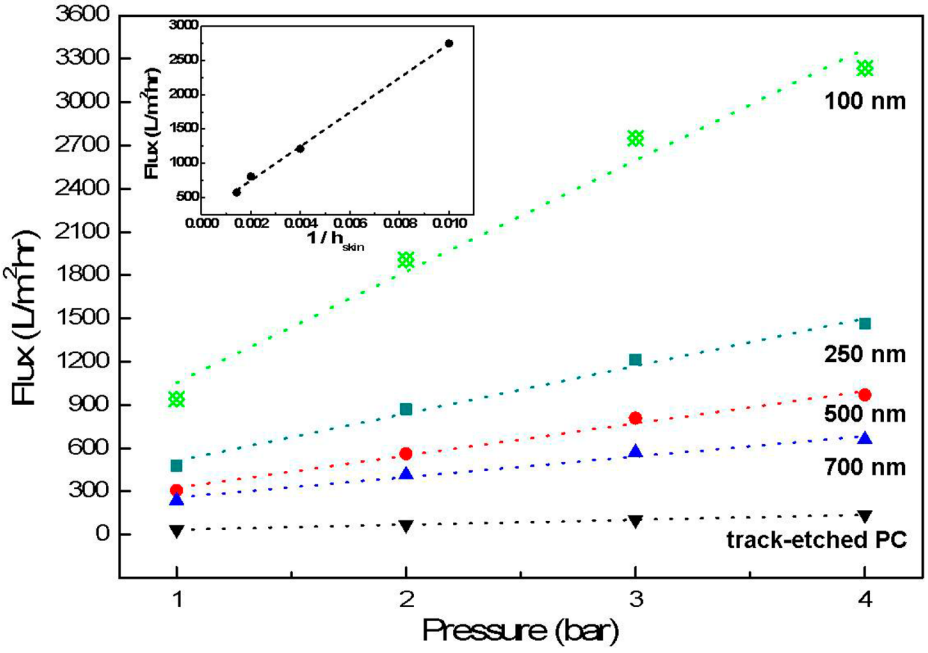


**Figure 3.** Plot of flux ($J$) versus applied pressure of the hierarchically self-organized monolithic nanoporous membranes having various thicknesses of the skin layer. Flux data for a track-etched PC membrane was added for the reference. Inset is plot of $J$ at 3 bar versus $1/h_{skin}$.

From Figure 3, $J$ of all of the membranes increased linearly with $\Delta P$. Also, at a given $\Delta P$, $J$ is inversely proportional to $h_{skin}$ (see the inset of Figure 3 at $\Delta P$ = 3 bar). The result is easily explained by the Hagen−Poiseuille equation for a membrane with cylindrical pores.[37]

$$J = \frac{{d_{pore}}^2 \varepsilon}{32\eta\tau}\frac{\Delta P}{h} \propto \frac{\Delta P}{h}$$

where $\varepsilon$ is the porosity of the film, $\eta$ is the viscosity of water, $\tau$ is the tortuosity of the pore, $h$ is the thickness of the membrane, and $d_{pore}$ is the diameter of pores. $J$ of the supporting layer is ∼4 times larger than that of the skin layer. This is because the pore size in the supporting layer is much larger (at least 20 times) than that in the skin layer, even though the thickness of the supporting layer is ∼700 times larger than that of the skin layer. Thus, the total flux is determined by the flux through the skin layer. Since $d_{pore}$, $\varepsilon$, $\eta$, and $\tau$ in the skin layer are identical for all the membranes employed in this study, $J$ is inversely proportional to $h_{skin}$ (see Section 3 in the Supporting Information).

Since the cleanness of a membrane prior to virus enrichment becomes very important to prevent contamination or damage to a virus by other biological pollutants, we performed a sterilization test by placing the membrane into a sterilizer maintained at 125 °C for 20 min. From SEM images of the nanoporous membrane before and after the sterilization (Figure S3 in the Supporting Information), the membrane exhibits excellent sterilizability because of using inorganic nanoporous membranes.

**Enrichment of HCV.** We used a hierarchically self-organized monolithic nanoporous membrane with a skin layer of 100 nm for the enrichment of HCV in stocks. Because of the hydrophilic surface of AAO membrane with a water contact angle of ∼30°, a little fouling was observed during the enrichment of HCV. The experimental details are described in the Experimental Section. Each concentration of HCV was measured with immunocytochemistry (ICC) analysis by counting the number of the foci (see Figure S4 of Section 5 in the Supporting Information). Therefore, in this study, only *infectious* HCV was counted. The efficiency of the HCV enrichment in stocks by the hierarchically self-organized monolithic nanoporous membrane and conventionally used centrifugation method is summarized in Figure 4. We used 100

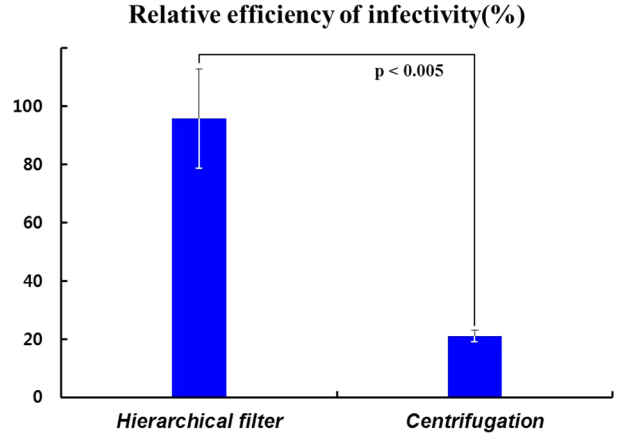


**Figure 4.** Efficiency of the *infectious* HCV enrichment in stocks by the hierarchically self-organized monolithic nanoporous membrane and conventionally used centrifugation method. $p$ is the correlation coefficient.

mL ($4.95 \times 10^4$ FFU/mL) of the original HCV supernatant. After this supernatant was filtered through the hierarchically self-organized monolithic nanoporous membrane, the remaining volume was reduced to 1 mL of supernatant. The *infectious* concentration of a hundred-fold enriched HCV was $4.62 \times 10^6$ FFU/mL (thus, the efficiency of 93.3% (average = 91.3%)). On the other hand, when the centrifugation method was used, the concentration of *infectious* HCV was $1.19 \times 10^6$ FFU/mL (thus, the efficiency of 24.0% (average = 22.0%)). Therefore, the

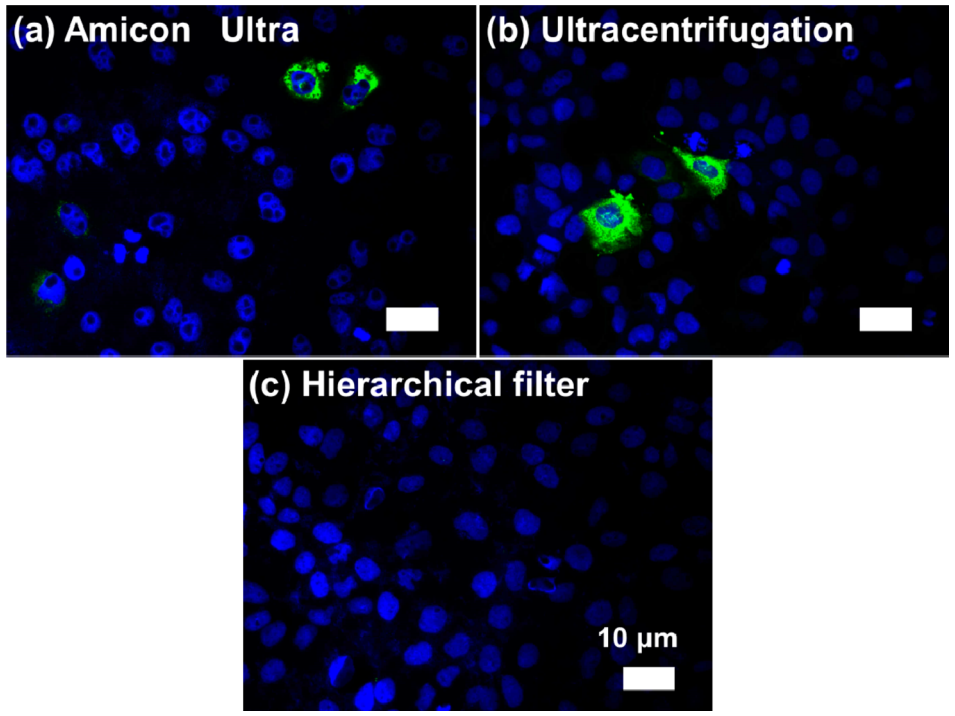


**Figure 5.** OM images of ICC experiment of discarded media treated human hepatoma cell line Huh 7.5.1 cells by various methods. (a) An ultrafiltration membrane (Amicon Ultra) under the centrifugation at a low rotating speed (3300 rpm), (b) ultracentrifugation at a very high rotating speed (36400 rpm), and (c) filtration by the hierarchically self-organized monolithic nanoporous membrane. Blue signal indicates the nucleus of human hepatoma cells, while green is the cells infected by HCV.

**Table 1. ICC Results of Enriched and Discarded HCV Supernatants by Using Centrifugation and Filtration with the Hierarchically Self-Organized Monolithic Nanoporous Membrane[a]**

| | | centrifugation | |
|---|---|---|---|
| original supernatant | | after the first step | after the second step |
| 100 mL, $4.95 \times 10^6$ FFU | concentrated supernatant | 27 mL, $3.56 \times 10^6$ FFU (72.0%) | 1 mL, $1.19 \times 10^6$ FFU (24.0%) |
| | discarded supernatant | 73 mL, $8.03 \times 10^4$ FFU (1.6%) | 26 mL, $6.24 \times 10^4$ FFU (1.3%) |
| | | filtration with the hierarchically self-organized monolithic nanoporous membrane | |
| | concentrated supernatant | 1 mL, $4.62 \times 10^6$ FFU (93.3%) | |
| | discarded supernatant | 99 mL, 0 FFU (0.0%) | |

[a]Volume, total number of foci.

efficiency of *infectious* HCV enrichment by hierarchically self-organized monolithic nanoporous membrane is four times higher than the centrifugation method.

Now, we consider why the centrifugation method gives low efficiency of HCV enrichment. Because we measured the *infectious* efficiency, two possibilities should be considered: the loss of HCV viruses and damage to HCV viruses during enrichment. The centrifugation method consists of two steps, as described in the Experimental Section. The first is to make the preconcentrated supernatant by using an ultrafiltration membrane (Amicon Ultra) under the centrifugation at a low rotating speed (3300 rpm). During this step, the volume of original supernatant (100 mL) in stocks is reduced to ~27 mL. The second step is to pelletize the HCV virion particles in the preconcentrated supernatant with ultracentrifugation at a very high rotating speed (36400 rpm). Then, HCV virus pellets are resuspended in 1 mL of media to make a high titer.

To check whether some HCV viruses existed in each discarded supernatant after the enrichment, we performed ICC analysis (Figure 5). As shown in Figure 5a,b, some HCV viruses are indeed observed in both discarded supernatants obtained by an ultrafiltration membrane under the centrifugation at a low rotating speed (3300 rpm) and ultracentrifugation at a very high rotating speed (36400 rpm), while the discarded supernatant after filtering original stock by using the hierarchically self-organized monolithic nanoporous membrane does not contain any HCV virus (Figure 5c).

However, the total amount of virus loss during each step of centrifugation method is found to be very small (less than ~2%), as shown in Table 1. This suggests that the low efficiency obtained by centrifugation is not due to the significant loss of HCV. Thus, we consider that the damage to the viruses during centrifugation would be the main reason. To check this possibility, we performed a real time polymerase chain reaction (PCR) of RNA in HCV, and the results are summarized in Table 2. The value obtained from real time PCR represents the amount of RNA copies in the supernatant regardless of infectivity of HCV viruses. As shown in Table 2, the total amount of RNA copies of the concentrated supernatants obtained by filtration with the hierarchically self-organized monolithic nanoporous membrane is similar to that obtained by centrifugation. On the other hand, the total

**Table 2. Total Amount of RNA Copies of Each Supernatant Measured by Real Time PCR after Enrichment of HCV Viruses in Stock by Using Two Methods**

| supernatant | total amount of RNA copies |
|---|---|
| original | $6.8 \times 10^{10}$ |
| centrifugation | |
| first step (Amicon Ultra) | $5.2 \times 10^{10}$ |
| second step (ultracentrifugation) | $3.3 \times 10^{10}$ |
| filtration with the hierarchically self-organized monolithic nanoporous membrane | $4.7 \times 10^{10}$ |

amount of *infectious* HCV is remarkably decreased during ultracentrifugation, as confirmed by the ICC result (see Table 1). We conclude that, though the amount of concentrated HCV virus particles after enrichment by centrifugation is similar to that obtained by filtration, severe damage to the HCV viruses occurs during ultracentrifugation. This is because HCV viruses could be easily damaged under the high pressure (or shear stress) during the ultracentrifugation.

## CONCLUSION

We fabricated a hierarchically self-organized monolithic nanoporous membrane using stepwise anodization on an aluminum sheet. The membrane consists of two layers: (1) a skin layer with thin thickness and regular pore size for perfect filtration and (2) a supporting layer with large pores for mechanical strength and high flux. We demonstrated that this membrane can be effectively used to concentrate HCV supernatant without the loss and damage of viruses. The efficiency of the concentration of HCV in stock was over 91%, which is greatly enhanced compared with that (~22%) obtained by the widely used centrifugation. A large reduction in the *infectious* efficiency obtained by centrifugation is due to the severe damage to HCV under the high pressure (or shear stress) exerted on HCV viruses during ultracentrifugation and pelletization. The membrane also shows excellent sterilizability because it is made of alumina. It could be effectively used in concentrating various fragile viruses in stocks such as rabies virus and human immunodeficiency virus in addition to HCV virus.

## ASSOCIATED CONTENT

### Supporting Information

Details of SEM images of various nanoporous membranes and membranes before and after sterilization, calculation of flux, and optical microscopy images of ICC results of concentrated HCV. This material is available free of charge via the Internet at http://pubs.acs.org.

## AUTHOR INFORMATION

### Corresponding Authors

*E-mail: sungkey@postech.ac.kr (S.K. Jang).
*E-mail: jkkim@postech.ac.kr (J.K. Kim).

### Author Contributions

†G.J. and M.J. contributed equally.

### Notes

The authors declare no competing financial interest.

## ACKNOWLEDGMENTS

This research was supported by the Bio R&D Program (No. 2012-054974) and the BRL (No. 2010-0019706) through the National Research Foundation funded by the MEST. This work was also supported by the National Creative Research Initiative Program of the National Research Foundation of Korea of the Ministry of Education, Science and Technology, Korea.

## REFERENCES

(1) Sanders, B. P.; Edo-Matas, D.; Custers, J.; Koldijk, M. H.; Klaren, V.; Turk, M.; Luitjens, A.; Bakker, W. A.; Uytdehaag, F.; Goudsmit, J.; Lewis, J. A.; Hanneke, S. *Vaccine* **2012**, *31*, 850−856.
(2) Kato, T.; Matsumura, T.; Heller, T.; Saito, S.; Sapp, R. K.; Murthy, K.; Wakita, T.; Liang, T. J. *J. Virol.* **2007**, *81*, 4405−4411.
(3) Park, J. H.; Jee, M. H.; Kwon, O. S.; Keum, S. J.; Jang, S. K. *Virology* **2013**, *439*, 13−22.
(4) Kim, C. S.; Keum, S. J.; Jang, S. K. *PLoS One* **2011**, *6*, No. e22808.
(5) Ploss, A.; Evans, M. J.; Gaysinskaya, V. A.; Panis, M.; You, H.; de Jong, Y. P.; Rice, C. M. *Nature* **2009**, *457*, 882−886.
(6) Dorner, M.; Horwitz, J. A.; Robbins, J. B.; Barry, W. T.; Feng, Q.; Mu, K.; Jones, C. T.; Schoggins, J. W.; Catanese, M. T.; Burton, D. R. *Nature* **2011**, *474*, 208−211.
(7) Zhong, J.; Gastaminza, P.; Cheng, G.; Kapadia, S.; Kato, T.; Burton, D. R.; Wieland, S. F.; Uprichard, S. L.; Wakita, T.; Chisari, F. V. *Proc. Natl. Acad. Sci. U.S.A.* **2005**, *102*, 9294−9299.
(8) Arifin, M. A.; Mel, M.; Karim, A.; Ismail, M.; Ideris, A. *J. Biomed. Biotechnol.* **2010**, *2010*, 1−7.
(9) Lawrence, J. E.; Steward, G. F. Purification of viruses by centrifugation. In *Manual of Aquatic Viral Ecology*; Wilhelm, S. W.; Weinbauer, M. G.; Suttle, C. A., Eds.; Association for the Sciences of Limnology and Oceanography: Waco, TX, 2010; p 166−181.
(10) Nuxoll, E. E.; Hillmyer, M. A.; Wang, R.; Leighton, C.; Siegel, R. A. *ACS Appl. Mater. Interfaces* **2009**, *1*, 888−893.
(11) Phillip, W. A.; O'Neill, B.; Rodwogin, M.; Hillmyer, M. A.; Cussler, E. *ACS Appl. Mater. Interfaces* **2010**, *2*, 847−853.
(12) Querelle, S. E.; Jackson, E. A.; Cussler, E. L.; Hillmyer, M. A. *ACS Appl. Mater. Interfaces* **2013**, *5*, 5044−5050.
(13) Losic, D.; Shapter, J. G.; Mitchell, J. G.; Voelcker, N. H. *Nanotechnology* **2005**, *16*, 2275−2281.
(14) Martin, C. R.; Siwy, Z. *Nat. Mater.* **2004**, *3*, 284−285.
(15) Yamaguchi, A.; Uejo, F.; Yoda, T.; Uchida, T.; Tanamura, Y.; Yamashita, T.; Teramae, N. *Nat. Mater.* **2004**, *3*, 337−341.
(16) Yang, S. Y.; Ryu, I.; Kim, H. Y.; Kim, J. K.; Jang, S. K.; Russell, T. P. *Adv. Mater.* **2006**, *18*, 709−712.
(17) Yang, S. Y.; Park, J.; Yoon, J.; Ree, M.; Jang, S. K.; Kim, J. K. *Adv. Funct. Mater.* **2008**, *18*, 1371−1377.
(18) Yang, S. Y.; Yang, J.-A.; Kim, E.-S.; Jeon, G.; Oh, E. J.; Choi, K. Y.; Hahn, S. K.; Kim, J. K. *ACS Nano* **2010**, *4*, 3817−3822.
(19) Yang, S. Y.; Son, S.; Jang, S.; Kim, H.; Jeon, G.; Kim, W. J.; Kim, J. K. *Nano Lett.* **2011**, *11*, 1032−1035.
(20) Peinemann, K.-V.; Abetz, V.; Simon, P. F. *Nat. Mater.* **2007**, *6*, 992−996.
(21) Nunes, S. P.; Behzad, A. R.; Hooghan, B.; Sougrat, R.; Karunakaran, M.; Pradeep, N.; Vainio, U.; Peinemann, K.-V. *ACS Nano* **2011**, *5*, 3516−3522.
(22) Phillip, W. A.; Mika Dorin, R.; Werner, J.; Hoek, E. M. V.; Wiesner, U.; Elimelech, M. *Nano Lett.* **2011**, *11*, 2892−2900.
(23) Jung, A.; Rangou, S.; Abetz, C.; Filiz, V.; Abetz, V. *Macromol. Mater. Eng.* **2012**, *297*, 790−798.
(24) Madhavan, P.; Peinemann, K.-V.; Nunes, S. P. *ACS Appl. Mater. Interfaces* **2013**, *5*, 7152−7159.
(25) Nielsch, K.; Müller, F.; Li, A.-P.; Gösele, U. *Adv. Mater.* **2000**, *12*, 582−586.
(26) Zhao, X.; Seo, S.-K.; Lee, U.-J.; Lee, K.-H. *J. Electrochem. Soc.* **2007**, *154*, C553−C557.
(27) Montero-Moreno, J.; Belenguer, M.; Sarret, M.; Müller, C. *Electrochim. Acta* **2009**, *54*, 2529−2535.
(28) Lee, D. Y.; Lee, D. H.; Lee, S. G.; Cho, K. *Soft Matter* **2012**, *8*, 4905−4910.
(29) Buijnsters, J. G.; Zhong, R.; Tsyntsaru, N.; Celis, J.-P. *ACS Appl. Mater. Interfaces* **2013**, *5*, 3224−3233.

(30) Kato, T.; Date, T.; Murayama, A.; Morikawa, K.; Akazawa, D.; Wakita, T. *Nat. Protoc.* **2006**, *1*, 2334−2339.
(31) Ravaggi, A.; Biasin, M. R.; Infantolino, D.; Cariani, E. *J. Virol. Methods* **1997**, *65*, 123−129.
(32) Masuda, H.; Fukuda, K. *Science* **1995**, *268*, 1466−1468.
(33) Masuda, H.; Yada, K.; Osaka, A. *Jpn. J. Appl. Phys.* **1998**, *37*, L1340−L1342.
(34) Li, A. P.; Müller, F.; Birner, A.; Nielsch, K.; Gösele, U. *Adv. Mater.* **1999**, *11*, 483−487.
(35) Chen, W.; Wu, J.-S.; Xia, X.-H. *ACS Nano* **2008**, *2*, 959−965.
(36) Lazzara, T. D.; Lau, K. A.; Abou-Kandil, A. I.; Caminade, A.-M.; Majoral, J.-P.; Knoll, W. *ACS Nano* **2010**, *4*, 3909−3920.
(37) Hayama, M.; Kohori, F.; Sakai, K. *J. Membr. Sci.* **2002**, *197*, 243−249.

## NOTE ADDED AFTER ASAP PUBLICATION

This paper was published on the Web on December 31, 2013, with inconsistent content describing the experimental parts for HCV Titer and HCV RNA. The corrected version was reposted on January 7, 2014.